Fracture Behavior of PVC/Blendex/Nano-$CaCO_3$ Composites

Ning Chen,[1] Chaoying Wan,[1] Yong Zhang,[1] Yinxi Zhang,[1] Changming Zhang[2]

[1]*Research Institute of Polymer Materials, Shanghai Jiao Tong University, Shanghai 200240, People's Republic of China*
[2]*Technical Center of Shanghai Chlor-Alkali Chemical Company, Shanghai 200241, People's Republic of China*

Received 12 September 2003; accepted 16 March 2004
DOI 10.1002/app.20786
Published online in Wiley InterScience (www.interscience.wiley.com).

ABSTRACT: PVC/Blendex/Nano-$CaCO_3$ composites were prepared by melt-blending method. The Blendex (BLENDEX® 338) (GE Specialty Chemicals Co., Ltd., Shanghai, China) was an acrylonitrile-butadiene-styrene copolymer with high butadiene content. The fracture behavior of PVC/Blendex/nano-$CaCO_3$ composites was studied using a modified essential work of fracture model, $U/A = u_0 + u_d l$, where u_0 is the limiting specific fracture energy and u_d is the dissipative energy density. The u_0 of PVC/Blendex blend could be greatly increased by the addition of nano-$CaCO_3$, while the u_d was decreased. Nano-$CaCO_3$ with particle size of 38 nm increased the u_0 of PVC/Blendex blend more effectively than that with particle size of 64 nm, when nano-$CaCO_3$ content was below 10 phr. Both the u_0 and u_d of PVC/Blendex/nano-$CaCO_3$ composites were not much affected by increasing specimen thickness from 3 mm to 5 mm, while the two fracture parameters were increased with increasing loading rate from 2 mm/min to 10 mm/min, and u_d was found to be more sensitive to the loading rate than u_0.
 J Appl Polym Sci 95: 953–961, 2005

Key words: poly(vinyl chloride) (PVC); calcium carbonate; composites; elastomers; fracture

INTRODUCTION

Particulate filled polymer nanocomposites have drawn intensive attention in recent years. Various nanoscale fillers, including montmorillonite,[1] silica,[2] calcium carbonate,[3–5] and aluminum oxide,[6] have been successfully used to improve the stiffness, toughness, and heat resistance of polymers. Among these fillers, calcium carbonate with nanoscale particle size (nano-$CaCO_3$) was one of the most commonly used spherical fillers in preparation of nanocomposites. It was reported that stearic acid surface-modified nano-$CaCO_3$ could remarkably improve the impact strength of polypropylene[3] and the heat resistance of polyethylene terephthalate.[4]

Polyvinyl chloride (PVC), as a commodity thermoplastic, has been widely used in industrial fields for many years. It has many good properties, such as low flammability, low cost, and formulating versatility, but its poor impact toughness and heat-softening temperature limit its application. A variety of elastomers have been developed to improve the impact toughness of PVC, such as acrylonitrile butadiene styrene copolymer (ABS). In this article, a modified ABS resin with high rubber content, Blendex (BLENDEX® 338), was used to toughen-modify PVC. Our previous study[7] showed that the Blendex was well compatible with PVC, and the notched impact strength of PVC/Blendex blends was much higher than that of pure PVC. After introduction of nano-$CaCO_3$, the impact resistance of PVC/Blendex blends can be further improved.

Izod and Charpy impact tests are the most commonly used methods in evaluation of the toughness of multiphase plastics. The two methods are quite convenient, but they are limited to specimens with a specific notch geometry and a given fracture area, and cannot give a general identification of the toughness of materials. Several fracture mechanics techniques, such as *J*-integral method, have come to be used. But the implementation of these techniques requires specialized equipment and rigorous treatment for specimens, which also limits their application to some extent.

The two-parameter methods developed by Vu-Khanh[8] and Mai[9] compromised the conventional Izod and Charpy impact tests and the rigorous *J*-integral method. They are easier to implement than *J*-integral method, and give more detailed information about material toughness than Izod and Charpy tests. According to Vu-Khanh, the energy (U) required to fracture ductile specimens with different ligament areas (A) is of the following form:

$$U/A = G_i + (T_a/2)A,$$

Correspondence to: Y. Zhang (yong_zhang@sjtu.edu.cn).

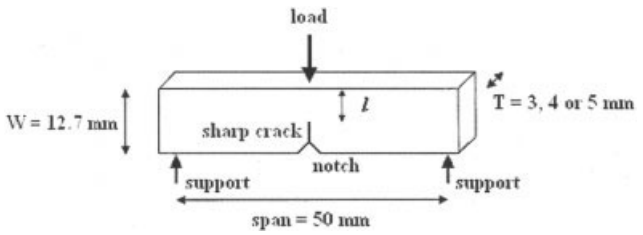

Figure 1 Schematic of SEN3PB specimen displaying width (W), thickness (T), and ligament length (l).

in which the intercept of a U/A versus A plot, G_i, is the fracture energy at crack initiation, and the slope, T_a, is the tearing modulus. The two parameters are suggested for characterization of impact toughness of ductile polymers. Measurements performed at a low loading rate demonstrate that G_i is in good agreement with the critical J-integral for fracture, J_{IC}.[8] For Mai's approach, also known as essential work of fracture (EWF) method, the total energy (W_f) absorbed by specimens with different ligaments (l) to fracture is of the following form:

$$W_f/lt = w_e + w_p\beta l,$$

in which t is the specimen thickness, w_e is the specific essential work of fracture, w_p is the specific nonessential work of fracture, and β is the shape factor of the plastic zone geometry. The intercept, w_e, and the slope, $w_p\beta$, of W_f/lt versus l plot are suggested to characterize the fracture behavior of ductile polymers.

There are some criteria that should be satisfied to apply the EWF method,[9] such as (a) each of the specimens must be deformed in the same fashion and (b) the specimen ligament must be fully yielded before crack growth. Actually, some of these criteria are difficult to be satisfied in the case of single edge-notched specimens or high loading rate. And this method is not appropriate if the two parts of the specimens could not be completely separated after testing. Okada and coworkers[10–12] proposed a modified model based on both Vu-Khanh and Mai's methods that can be expressed as following:

$$U/A = u_o + u_d l,$$

in which u_0 is the limiting specific fracture energy that represents the energy required to create a unit area of fracture surface, and u_d is the dissipative energy density that reflects the plastic deformation energy in the process zone surrounding the fracture surface. Unlike w_e and $w_p\beta$, u_0 and u_d are defined as phenomenological parameters. Therefore, eq. (3) can be used in some conditions where EWF method is not suitable.

In this article, the suitability of EWF method for the study of the fracture behavior of PVC/Blendex/nano-$CaCO_3$ composites is discussed. The effects of the content and particle size of nano-$CaCO_3$, specimen thickness and loading rate on the fracture behavior of the composites were studied. The fracture patterns of the composites were also observed.

EXPERIMENTAL

Materials and sample preparation

Suspension PVC (WS-800, $\overline{DP}$ = 800) was produced by Shanghai Chlor-Alkali Chemical Co., Ltd., Shanghai, China. BLENDEX® 338, a butadiene-styrene-acrylonitrile impact modifier resin with 70% butadiene content, was produced by GE Specialty Chemicals Co., USA. Nano-$CaCO_3$, including s-$CaCO_3$ and l-$CaCO_3$ (distinguished by particle size), was surface-modified with stearic acid and produced by Shanghai Perfection Nanometre New Material Co., Ltd., Shanghai, China. The organic tin stabilizer and stearic acid were industry grade products.

PVC 100 phr, Blendex 20 phr, organic tin stabilizer 5 phr, and stearic acid 0.3 phr were premixed together in a high-speed mixer for 8 min to give PVC compound. Nano-$CaCO_3$ was dried at 80°C for 24 h in a vacuum oven. The PVC compound and nano-$CaCO_3$ were melt-mixed on a two-roll mill at 170°C for 10 min to give composites. The composites thus prepared were molded into sheets of 3, 4, and 5 mm in thickness by compression-molding at 180°C and 20 MPa for 10 min, followed by cooling to room temperature at 10MPa.

Characterization

Three-point-bending tests were performed on an Instron 4465 Universal Tensile Tester (England). The

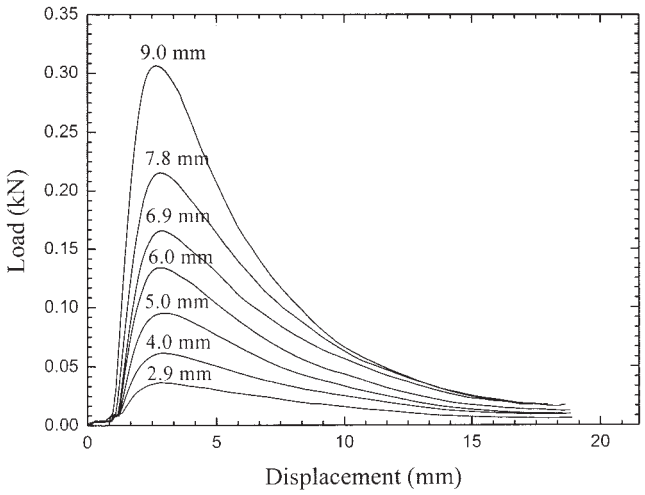

Figure 2 Load-displacement curves for specimens of PVC/Blendex/s-$CaCO_3$ (100/20/10) composite of different ligament lengths.

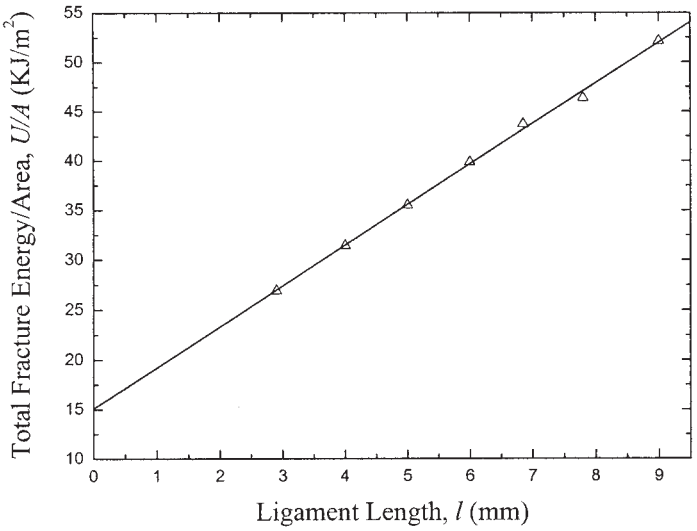

Figure 3 U/A versus l curves for PVC/Blendex/s-$CaCO_3$ (100/20/10) composite.

single-edge notched three-point bending (SEN3PB) specimens (Fig. 1) were cut from the compression-molded sheets. The length of initial crack consisted of the length of machined notch and the sharp crack length created by pushing a sharp razor blade into the tip of machined notch. The ligament length l was measured from the original crack tip to the beginning of the hinge. The loading rate varied from 2 mm/min to 10 mm/min.

The composites were ultrathin-sectioned using a Reichert-jung Ultracut E microtome (Westmont, NJ). The sections (about 100 nm) were mounted on copper grids and observed by transmission electron microscopy (TEM) using a JEM-1200EX apparatus (Tokyo, Japan) running at an acceleration voltage of 80 KV. The facture surfaces of composites were observed by scanning electron microscopy (SEM) with a Hitachi-*S*-2150 apparatus (Tokyo, Japan) running at an acceleration voltage of 20 KV. The surfaces were covered by gold prior to observation.

RESULTS AND DISCUSSION

Determination of fracture parameters

Figure 2 shows the typical load-displacement curves for the specimens of PVC/Blendex/s-$CaCO_3$ (100/20/10) composite of various ligament lengths. The loading rate was 2 mm/min and the specimens were 4 mm in thickness. In Figure 2, the load-displacement curves for all ligament lengths are geometrically similar, suggesting that the specimens of different ligament lengths were deformed in the same mode. Thus, the EWF criterion (a) is satisfied. However, it was found that for all specimens the crack propagated before full ligament yielding, and the two parts of the specimens could not be completely separated after testing. There-

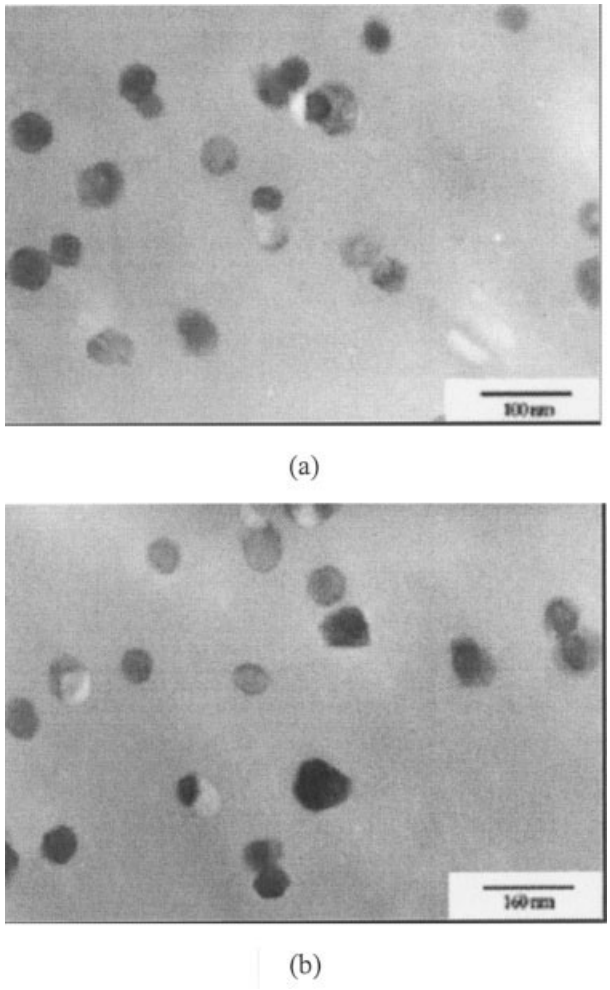

Figure 4 TEM photographs for (a) PVC/Blendex/s-$CaCO_3$ (100/20/10) and (b) PVC/Blendex/l-$CaCO_3$ (100/20/10) composites.

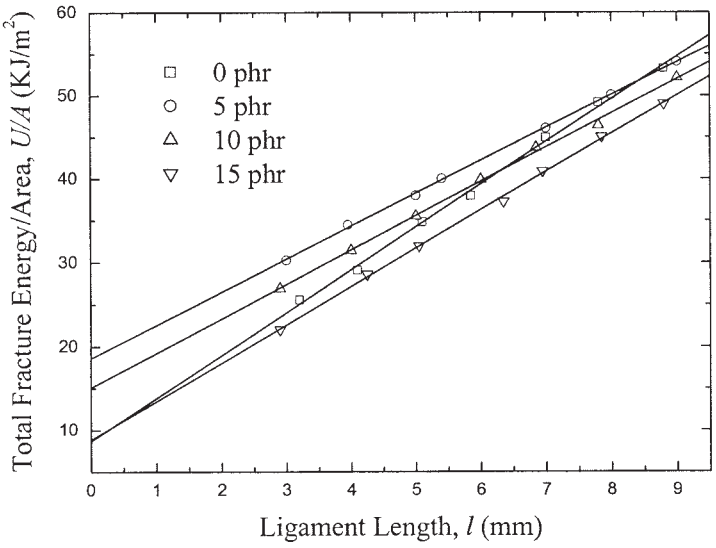

(a)

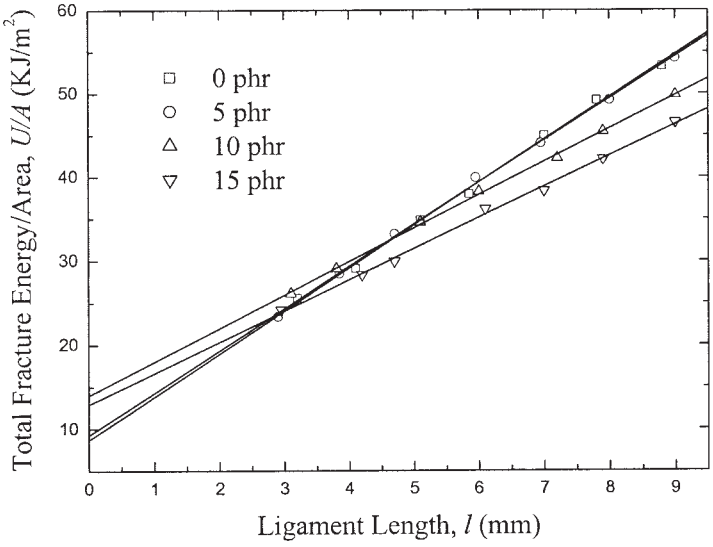

(b)

Figure 5 *U/A* versus *l* curves for (a) PVC/Blendex/*s*-$CaCO_3$ and (b) PVC/Blendex/*l*-$CaCO_3$ composites with different $CaCO_3$ contents.

fore, the concept of EWF is not appropriate in this case. The modified EWF method, eq. (3), was chosen to characterize the fracture behavior of PVC/Blendex/nano-$CaCO_3$ composites in the following. Since the two parts of the specimens could not be completely separated, the ligament length *l* was measured with the length of crack that virtually propagated.

The total fracture energy *U* was calculated from the integrated area under the load-displacement curves and the data represented as *U/A* versus *l* for the composite are shown in Figure 3. The *U/A* versus *l* displays good linearity, and the fracture parameters, u_0 and u_d, are finally obtained.

Effects of content and particle size of nano-$CaCO_3$

To evaluate the effects of content and particle size of nano-$CaCO_3$ on the fracture behavior of the composites, the fracture parameters of composites based on

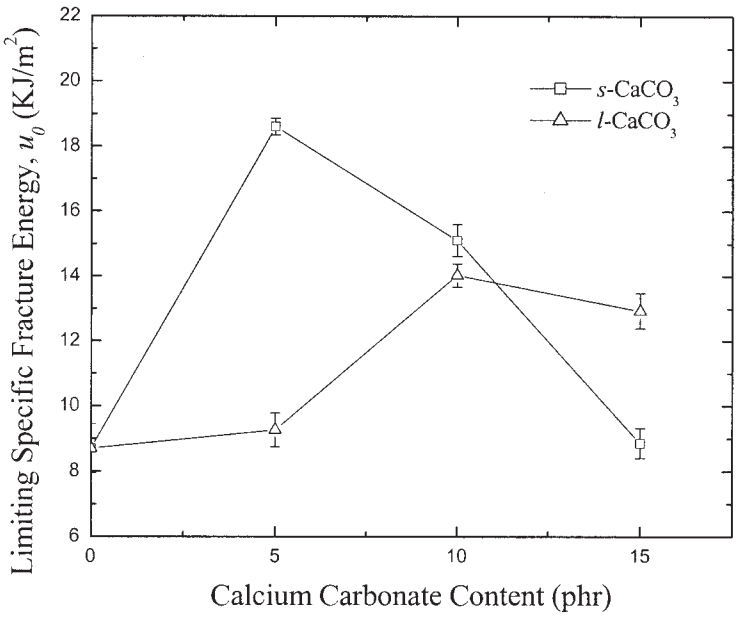

(a)

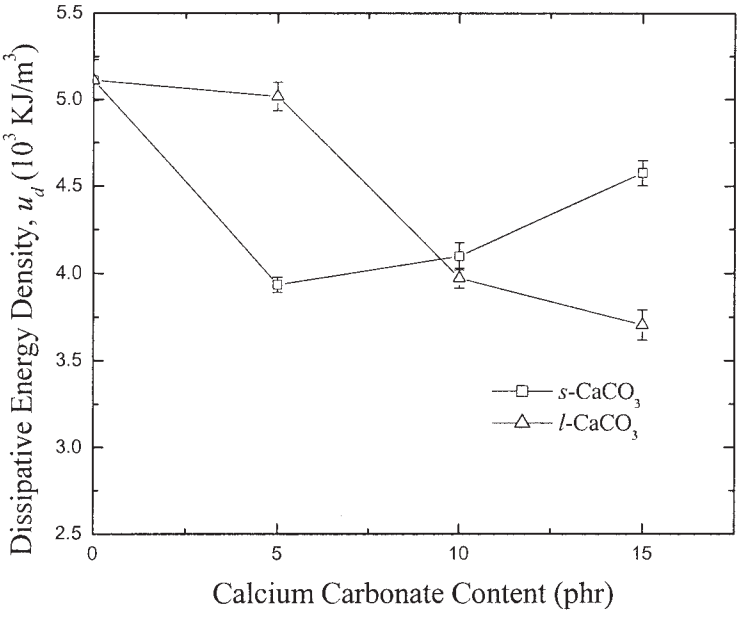

(b)

Figure 6 (a) u_0 and (b) u_d for PVC/Blendex/*s*-$CaCO_3$ and PVC/Blendex/*l*-$CaCO_3$ composites as a function of $CaCO_3$ content.

two kinds of nano-$CaCO_3$ of different particle size with the filler content varying from 0 to 15 phr were determined. The loading rate was 2 mm/min and the specimens were 4 mm in thickness.

Figure 4 reveals that both of the two kinds of nano-$CaCO_3$ are uniformly dispersed in PVC/Blendex matrix. The average particle sizes of about 38 nm and 64 nm are obtained for *s*-$CaCO_3$ and *l*-$CaCO_3$, respec-

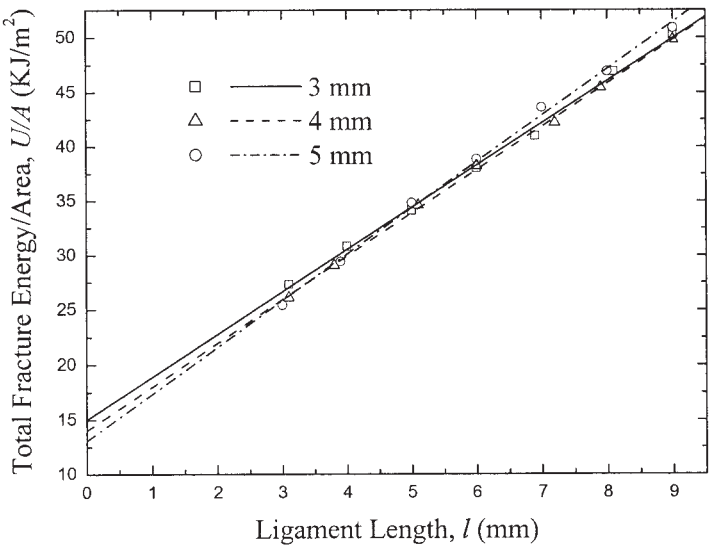

Figure 7 *U/A* versus *l* curves for PVC/Blendex/*l*-$CaCO_3$ (100/20/10) composite of different specimen thickness.

tively, by measuring the sizes of 20 randomly chosen particles.

The *U/A* versus *l* plots of the composites are shown in Figure 5. Each of them displays good linearity. The fracture parameters were calculated and shown in Figure 6. It can be observed that, independent of particle size of the filler, the u_0 of PVC/Blendex blend was greatly increased by the introduction of nano-$CaCO_3$ when the filler content was below 10 phr, while the u_d is considerably decreased. The net result of these contrary effects is that PVC/Blendex has higher fracture energy at long ligament, whereas the composites containing a proper content of nano-$CaCO_3$ have much higher fracture energy at short ligament (Fig. 5). These contrary effects were also reported by Laura and coworkers[12] for nylon 6/maleated ethylene-propylene/glass fiber composites.

Another important observation from Figure 6 is that the u_0 of PVC/Blendex/*s*-$CaCO_3$ composites is much larger than that of PVC/Blendex/*l*-$CaCO_3$ composites when the $CaCO_3$ content is below 10 phr. For example, the u_0 of PVC/Blendex/*s*-$CaCO_3$ composites reaches

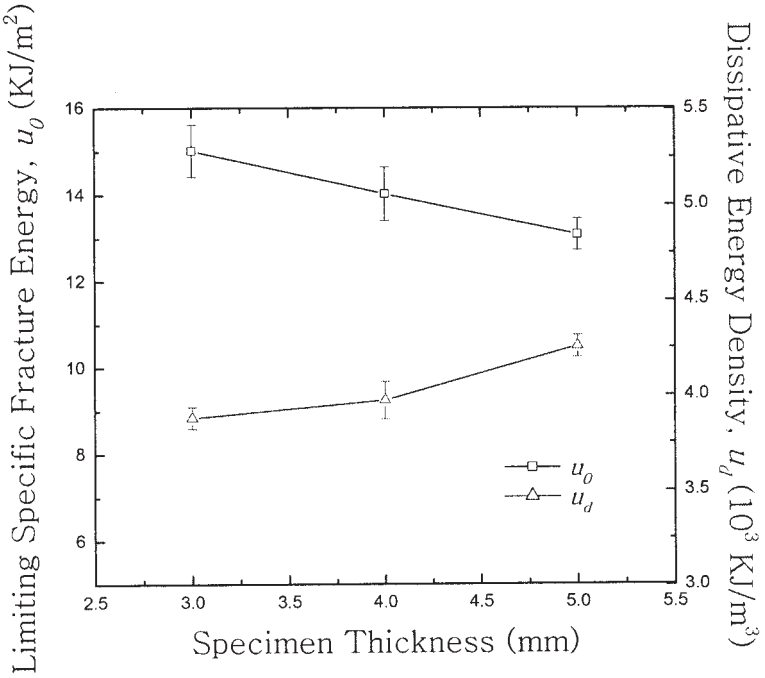

Figure 8 u_0 and u_d for PVC/Blendex/*l*-$CaCO_3$ (100/20/10) composite as a function of specimen thickness.

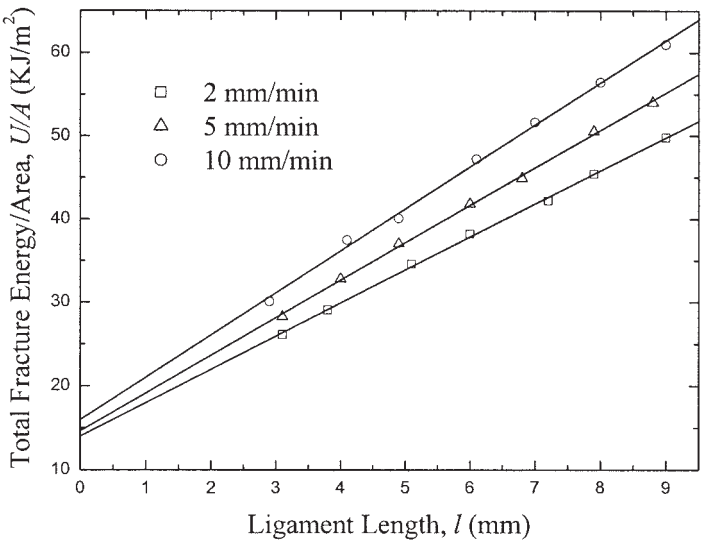

Figure 9 *U/A* versus *l* curves for PVC/Blendex/*l*-$CaCO_3$ (100/20/10) composite of different loading rate.

its peak value of 18.60 KJ/m^2 when 5 phr of *s*-$CaCO_3$ is introduced, which is about 10 times larger than that of PVC/Blendex matrix, that is, 8.69 KJ/m^2. However, the u_0 of the PVC/Blendex/*l*-$CaCO_3$ composite peaks only at 14.02 KJ/m^2 when 10 phr of *l*-$CaCO_3$ is added. In particular, at a given $CaCO_3$ content of 15 phr, the u_0 of PVC/Blendex/*s*-$CaCO_3$ composites is much lower than that of PVC/Blendex/*l*-$CaCO_3$ composites. One possible reason for this phenomenon is that *s*-$CaCO_3$ has smaller particle size and tends to aggregate in comparison with *l*-$CaCO_3$, which may result in the u_0 of PVC/Blendex/*s*-$CaCO_3$ composites being more sensitive to the *s*-$CaCO_3$ concentration increase.

It can also be seen from Figure 6 that the u_d of PVC/Blendex/*s*-$CaCO_3$ composites is minimized when 5 phr $CaCO_3$ is introduced, while that of PVC/Blendex/*l*-$CaCO_3$ composites is decreased in general with increasing the filler content.

Effects of specimen thickness and loading rate

The fracture behavior of polymers is known to be related to the specimen size and loading rate, which basically involve the size and time effects. To estimate the effects of specimen size and loading rate on the

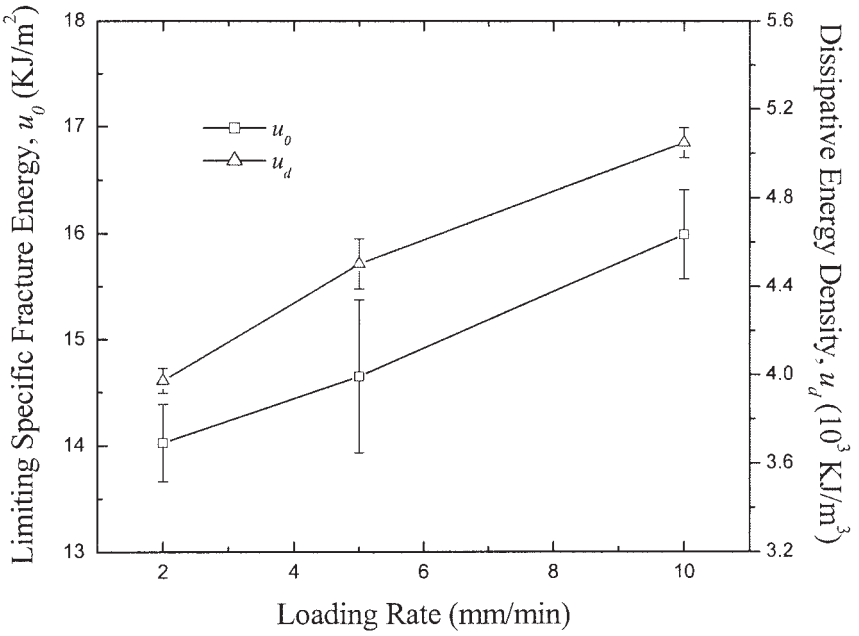

Figure 10 u_0 and u_d for PVC/Blendex/*l*-$CaCO_3$ (100/20/10) composite as a function of loading rate.

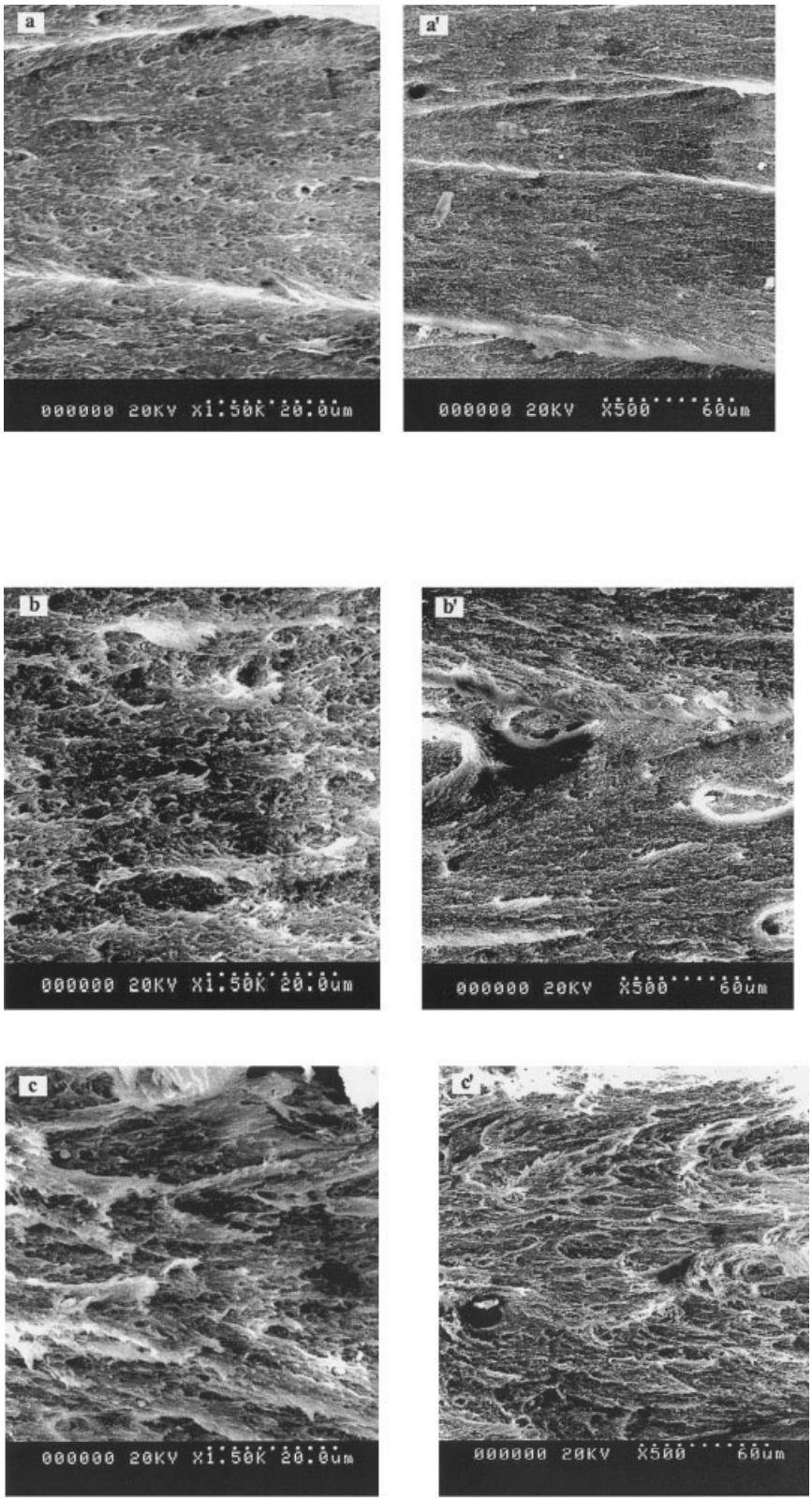

Figure 11 SEM photographs for the fracture surfaces of (a) and (a′) PVC/Blendex blend (specimen thickness is 4 mm, loading rate is 2 mm/min); (b) and (b′) PVC/Blendex/*l*-$CaCO_3$ (100/20/10) composite (specimen thickness is 4 mm, loading rate is 2 mm/min); and (c) and (c′) PVC/Blendex/*l*-$CaCO_3$ (100/20/10) composite (specimen thickness is 4 mm, loading rate is 10 mm/min).

behavior of the composites, the fracture parameters of PVC/Blendex/*l*-$CaCO_3$ (100/20/10) composite as a function of specimen thickness and loading rate were examined respectively.

Figure 7 displays *U/A* versus *l* plots for the composite of different specimen thickness. Figure 8 shows the fracture parameters as a function of specimen thickness. It can be seen that the fracture parameters of the composite are not much affected by specimen thickness. With increasing specimen thickness from 3 mm to 5 mm, the u_0 of the composite is decreased by 12.8%, and the u_d is only increased by 9.7%.

Figures 9 and 10 display the *U/A* versus *l* plots of the PVC/Blendex/*l*-$CaCO_3$ (100/20/10) composite and the fracture parameters at different loading rate, respectively. As shown in Figure 10, the u_0 and u_d of the composite are increased with increasing loading rate, and the u_d is found to be more sensitive to loading rate than the u_0. With increasing loading rate from 2 mm/min to 10 mm/min, the u_0 is increased by 14%, while the u_d is increased by about 27%.

Fracture surface observation

Figure 11 reveals the SEM photographs of the fracture surfaces of PVC/Blendex blend and PVC/Blendex/nano-$CaCO_3$ composites. Several long shearing bands are parallelized to each other and a low degree of cavitation emerges on the fracture surface of PVC/Blendex blend, indicating that the PVC/Blendex blend fractures in a ductile mode. A high degree of cavitation is found on the fracture surface of the PVC/Blendex/*l*-$CaCO_3$ (100/20/10) composite. Meanwhile, the shearing bands become quite short and less orientational, and some shallow basins edged with shearing bands can be observed. It also can be seen from Figure 11(b) that many nano-$CaCO_3$ particles were separated from the matrix. All these phenomena suggest that more energy would be needed to create a unit area of fracture surface for the PVC/Blendex/*l*-$CaCO_3$ composites than the PVC/Blendex blend, leading to the increase of u_0. As shown in Figures 11c) and (c'), the fracture surface of the PVC/Blendex/*l*-$CaCO_3$ composites created at a higher loading rate is much coarser. Obviously, this kind of fracture surface dissipates more energy, and leads to a higher u_0.

CONCLUSION

The EWF method was not appropriate for studying the fracture behavior of PVC/Blendex/nano-$CaCO_3$ composites by SEN3PB tests, but the modified EWF method, $U/A = u_0 + u_d l$, fit experiment data well. The limiting specific fracture energy, u_0, of PVC/Blendex blend could be greatly increased by the introduction of nano-$CaCO_3$, while the dissipative energy density, u_d, was considerably decreased. Nano-$CaCO_3$ of smaller particle size could increase the u_0 of PVC/Blendex blend more effectively than that with larger size at low $CaCO_3$ content. The facture parameters of PVC/Blendex/nano-$CaCO_3$ composites were not much affected by increasing specimen thickness from 3 mm to 5 mm. Both the u_0 and u_d of the composites were increased with increasing loading rate, and the u_d was more sensitive to loading rate than the u_0.

References

1. Wan, C. Y.; Zhang, Y.; Zhang, Y. X.; Qiao, X. Y.; Teng, G. M. J Polym Sci: Polym Phy 2003, to appear.
2. Reynaud, E.; Jouen, T.; Gaunthier, C.; Vigier, G.; Varlet, J. Polymer 2001, 42, 8759.
3. Chan, C. M.; Wu, J. S.; Li, J. X.; Cheung, Y. T. Polymer 2002, 43, 2981.
4. Di Lorenzo, M. L.; Errico, M. E.; Avella, M. J Mater Sci 2002, 37, 2351.
5. Avella, M.; Errico, M. E.; Martuscelli, E. Nano Letters 2001, 1, 213.
6. Cao, Y. M.; Sun, J.; Yu, D. H. J App Polym Sci 2002, 83, 70.
7. Chen, N.; Wan, C. Y.; Zhang, Y.; Zhang, Y. X. Polym Test 2003, to appear.
8. Vu-Khanh, T. Polymer 1988, 29, 1979.
9. Mai, Y. W.; Powell, P. J Polym Sci: Polym Phy 1991, 29, 785.
10. Kudva, R. A.; Keskkula, H.; Paul, D. R. Polymer 2000, 41, 335.
11. Okada, O.; Keskkula, H.; Paul, D. R. Polymer 2000, 41, 8061.
12. Laura, D. M.; Keskkula, H.; Barlow, J. W.; Paul, D. R. Polymer 2001, 42, 6161.